DEUTSCHES ELEKTRONEN-SYNCHROTRON DESY

DESY 88-014
February 1988

SOFT PROCESSES IN VERY HIGH ENERGY PROTON-PROTON COLLISIONS

by

G. Ingelman

Deutsches Elektronen-Synchrotron DESY, Hamburg

ISSN 0418-9833

NOTKESTRASSE 85 · 2 HAMBURG 52

To be sure that your preprints are promptly included in the
HIGH ENERGY PHYSICS INDEX ,
send them to the following address (if possible by air mail) :

DESY
Bibliothek
Notkestrasse 85
2 Hamburg 52
Germany

DESY 88-014
February 1988

ISSN 0418-9833

Soft Processes in Very High Energy Proton-Proton Collisions [1]

G. Ingelman
Deutsches Elektronen-Synchrotron DESY
Notkestrasse 85, D-2000 Hamburg 52, FRG

Abstract

Soft processes in terms of fragmentation of high-$p_\perp$ and low-$p_\perp$ jets are considered in relation to the high and low momentum transfer mechanisms that produce them. The evolution of high-$p_\perp$ jets can be reliably described based on perturbative QCD radiation and hadronization models tuned at present energies and we give realistic predictions for the properties of such jets at very high energies. The modelling of low-$p_\perp$ spectator jets and minimum bias events, on the other hand, involve important uncertain elements regarding the interaction mechanism and the resulting colour field structure which lead to large uncertainties in the resulting predictions. Diffractive scattering is discussed in terms of the nature of the pomeron and its interactions, in particular the possibility of parton constituents in the pomeron and 'hard diffractive scattering' is considered.

1 Introduction

The notion of 'soft' process is not quite well defined and when extrapolating to the enormous energies that the ELOISATRON would provide one has to first discuss its meaning, e.g. whether 'soft' is to be understood on an absolute or relative scale. Usually a limited absolute scale in transverse momentum exchange of the order 1 GeV is thought of, and this will also be our attitude. A scale increasing with total energy, $\sqrt{s}$, would mean that many processes which are presently successfully described as hard would be classified as soft at future high energy machines. One should note, however, that the requirement of a low *transverse* momentum exchange does not exclude the occurence of substantial *longitudinal* momentum transfers. There are in fact models for minimum bias interactions that involve such longitudinal momentum exchanges, either explicitly by construction or implicitly. Another aspect is that processes or objects that occur as hard processes at lower energies may also arise through soft processes at larger energies. An example is provided by charm production which seems to be explained by hard QCD fusion processes at fixed target energies, but may have an important diffractive component at ISR energies. Another case is W and Z bosons which appear in hard processes at present collider energies, but in some circumstances can be treated by a Weizäcker-Williams 'equivalent boson' approximation at supercollider energies. The recent discussion on 'minijets' and their possible relation to the total cross-section rise, also illustrate the vague borderline between 'hard' and 'soft' physics with increasing energy.

There is thus an important interplay between the 'hard' and 'soft' physics that we might associate with the parton and hadron 'worlds', respectively. In the ultimate theory these aspects will be related, presumably by colour confinement which today is a major unsolved problem in high energy hadron physics. It is only due to our present ignorance and limited calculational techniques, e.g. perturbation theory, that 'hard' and 'soft' physics are treated separately. To improve our understanding it is, therefore, interesting to investigate the relations between our present theories and models for hard and soft interactions. This is of importance also for practical reasons of planning future experiments, namely in order to make realistic predictions of what events will look like at supercollider energies.

Although soft processes also include important issues like total cross-sections, elastic and diffractive scattering, this will not be discussed here. The only exception is the possibility of a parton structure in the pomeron and its consequences in terms of so-called 'hard diffractive scattering'. The organization of the paper is as follows. The properties of high-$p_\perp$ jets resulting from perturbative jet evolution and non-perturbative hadronisation is discussed in Section 2, whereas Section 3 considers low-$p_\perp$ jets in the sense of beam jets and minimum bias interactions. In Section 4 some ideas on pomeron structure and interactions are discussed and, finally, we end with some concluding remarks in Section 5.

2 Hard and soft components in high-$p_\perp$ jets

The properties of high-$p_\perp$ jets are influenced both by hard, or semihard, parton processes that can be calculated in perturbative QCD and by soft hadronization processes of a non-perturbative QCD origin which cannot be calculated from fundamental principles at present. Phenomenologically successful models for the latter exists and to the extent that these are not just parametrizations of data, but rather based on more or less elaborate physics ideas, they can have a large predictive power leading to useful tests of the assumptions involved in the models. The use of a separate treatment of the pertubative and non-perturbative phases is based on the assumption that they occur sequentially with two sufficiently well separated space-time scales. Nevertheless, the two parts must be properly connected and our attempts to understand high-$p_\perp$ jets in detail thus involve an interplay of 'hard' QCD theory and 'soft' models and can thereby serve as a suitable test bench for our purposes.

[1] Invited talk at the INFN workshop on Very High Energy Proton-Proton Physics, Erice, Italy, May 31 - June 7, 1987.

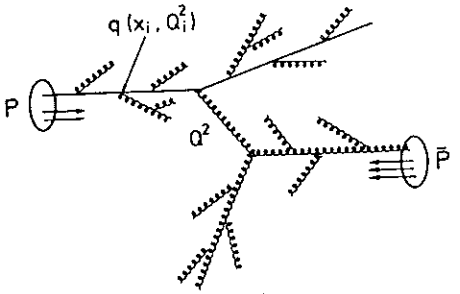

Figure 1: *Initial and final state parton radiation in high-$p_\perp$ hadron-hadron scattering.*

2.1 Perturbative jet evolution

The calculation of matrix elements in QCD perturbation theory is well defined, but quickly becomes very complicated for higher order processes. In high-$p_\perp$ hadron-hadron scattering exact matrix elements have been calculated up to order α_s^4 [1], corresponding to at most four partons in the final state (spectators not counted). Still higher order diagrams, giving rise to multiparton final states, are important not only at higher energies, but also at present energies in order to understand detailed jet evolution properties. This requires the use of approximation schemes and the parton cascade approach (for a review see [2]) is particularly useful since the complete final parton state can be dynamically simulated on a computer giving access to all possible variables. The basic idea is that partons emitted in a large transverse momentum process can be off mass shell and emit bremsstrahlung gluons, which may in turn split into gluon or $q\bar{q}$ pairs, leading to a shower of partons as illustrated in Fig. 1.

Parton cascade models have been developed to a high degree over the last few years [3,4,5]. The common feature of such models is that first order QCD matrix elements in the leading logarithm approximation is used for each separate branching, i.e. the Altarelli-Parisi equations [6] for the basic perturbative splitting processes $q \to qg$, $g \to gg$ and $g \to q\bar{q}$ are used in an iterative procedure which is stopped when all parton virtualities, m_i^2, are below a cutoff, t_{cut}, usually chosen of order 1 GeV^2. Together with Λ_{QCD} this cutoff regulates the amount of partons radiated. One should bear in mind that this approximation is not expected to work properly for hard gluon emission at large angles where interferences between diagrams with the gluon emitted from different parton lines are important. These models are rather intended for studies of e.g. jet broadening due to the emission of several but not very hard gluons at large angles. Nevertheless, these models may be used also for multiple jet phenomena simply because better higher order calculations are lacking at present; the general features will certainly be adequately described although the rates and some distributions will not be exactly the correct ones.

In a high-$p_\perp$ proton-proton collision, Fig. 1, the scattered partons may have a virtual mass squared up to order Q^2 and produce final state parton emission of a timelike character, i.e. all partons have $m^2 \geq 0$, which can be described by models developed for e^+e^- annihilation. This usually involves an angular ordering to take

interferences between soft gluons into account [4] and very good agreement with experimental data can be obtained [7]. In hadron collisions, however, not only the scattered parton, but also the partons entering the hard scattering process can emit radiation, Fig. 1. In this case, the radiating parton develops a negative virtuality, i.e. has a space-like 4-vector giving $m^2 < 0$. This initial state cascade evolution may be viewed as a quantum fluctuation which can only be realized in a large momentum transfer process which put the parton back on shell or to a positive virtuality, i.e. $m_i^2 < 0 \rightsquigarrow m_f^2 \geq 0$. For practical reasons it is better to start with the hard scattering, given by the $2 \to 2$ exact matrix elements, and perform the initial cascade evolution backwards in time. Such a scheme, developed in [8], must also take into account constraints from the structure functions, since at each intermediate step one should have the correct probability of finding a parton with momentum fraction x_i at the proper momentum transfer scale Q_i^2 as indicated in Fig. 1. This leads to a modified splitting probability

$$dP_b = |dt| \, \frac{\alpha_s(Q^2)}{2\pi} \sum_a \int \frac{dx'}{x'} \, \frac{f_a(x',t)}{f_b(x,t)} \, P_{a\to bc}\left(\frac{x}{x'}\right) \qquad (1)$$

with the ratio of the structure functions, f, before and after splitting as a weight. Otherwise the procedure is similar to that of final state radiation. The structure functions, however, has the effect of reducing the amount of radiation as compared to the case for final state radiation. For the properties of high-$p_\perp$ jets the initial state radiation is of less importance, but it does influence the underlying event and also generate a transverse momentum of the hard scattering system.

Although the parton shower approach is phenomenologically very useful, one should realize its limitations. Not only does it involve the QCD leading log approximation, but also some details which are not theoretically well-defined. It cannot, therefore, replace exact matrix element calculations for fundamental tests of QCD and the determination of Λ_{QCD} in a well-defined renormalization scheme. Ideally one would use exact matrix elements up to the order available and then add the higher order effects by a cascade model. This give rise, however, to problems of a proper joining of the two methods such that double counting is avoided; so far this is only solved for order α_s matrix elements in e^+e^- annihilation [5]. Furthermore, α_s used in each separate branching depends on the momentum transfer in that vertex, and therefore becomes larger the further the cascade is evolved and the perturbative approximation will break down at some point when the parton virtualities become small. The value for the parameter t_{cut}, which determines the border line between the region where perturbative QCD can be considered trustworthy and the following non-perturbative region, is not given by theory but is basically a free parameter which is obtained from comparison with data after a method for the final hadronization step has been included.

2.2 Non-perturbative hadronization

The simplest fragmentation model where all partons from the shower hadronize independently of each other using, e.g., the Field-Feynman parametrization [9] is not stable with respect to changes of this t_{cut} value [10] and is therefore not suitable. Being essentially a parametrizatiuon it is furthermore not so interesting since it does not

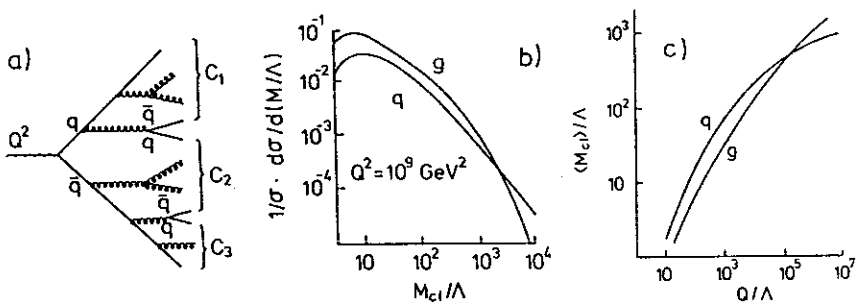

Figure 2: *(a) Preconfinement of perturbatively produced quanta into colour singlet clusters. (b) Cluster mass distribution at asymptotic energy. (c) Average mass versus energy scale. Energies and masses are scaled with Λ_{QCD}; q and g refer to quark and gluon jet, respectively. From [12].*

provide much understanding. Physically more interesting is the possibility of cluster formation from the partons and, in particular, the idea of preconfinement [11]. Given the well-defined colour ordering of the planar graph the partons can be associated with colour singlet clusters (Fig. 2a) which could form a link to the hadronic final state. Considering e^+e^- annihilation for simplicity, the original $q\bar{q}$ colour singlet system can give rise to more than one cluster only if additional $q\bar{q}$ pairs are formed in the perturbative shower evolution. Consequently, the cluster multiplicity and mass spectrum depends on the frequency of the $g \to q\bar{q}$ branching. Analytical calculations in an asymptotic limit indicates that the typical cluster mass is close to the shower cutoff, i.e. close to the hadronic mass scale, and, moreover, essentially independent of Q^2 [11]. More detailed investigations based on Monte Carlo simulations show that this is not quite correct [12]. The mass spectrum of such clusters, Fig. 2b, has indeed a peak at small masses, but also a long tail to large masses which makes the average mass quite appreciable and also increasing with increasing Q^2, Fig. 2c. The cluster masses are therefore in reality significantly above the hadron mass scale and become even more so at higher energy scales. Unfortunately, this prevents an easy connection between perturbatively produced clusters and the final state hadrons.

Nevertheless, it is possible to construct phenomenological cluster models [4] by first splitting the gluons into $q\bar{q}$ pairs and then let colour-connected $q\bar{q}$ pairs form lower mass clusters, which are finally decayed into ordinary hadrons (including resonances) using pure phase space. The continous cluster mass spectrum obtained will obviously depend on the parton shower cutoff value and hence a low cutoff is preferable in order to get cluster masses not too much above the hadron mass scale. Even with a small cutoff, however, large mass clusters will occur and their isotropic phase space decay will produce too spherical events compared to e^+e^- data. This is usually solved by splitting heavy clusters, with a mass larger than 3–4 GeV, into lower mass clusters using a longitudinal (string-like) decay.

Another approach is to connect the perturbatively produced partons, whose colour ordering is given by the shower evolution, with a colour string force field and apply the Lund fragmentation model [13] for the final hadronization step. A colour triplet and antitriplet charge, e.g. q and $\bar{q}$, are here represented by the endpoints and a

Figure 3: *(a) Representation of a $q\bar{q}g$ system using a triplet string stretched via the colour octet gluon. The velocity of a string piece is $v = \cos\theta/2$. (b) Alternative gluon model with a colour octet string joining the two triplet strings at a junction.*

gluon colour octet charge by an energy-momentum carrying kink on the string, Fig. 3a. Thus, a rather complicated string topology arise when many gluons have been emitted. The string model provides a desired stability [10,14], of the final hadron state properties with respect to variations of the arbitrary t_{cut} parameter since the extra gluons emitted with a lower cutoff will only produce small disturbances on the string configuration obtained without them. In e^+e^-, e.g., more than one colour string system will only occur if $q\bar{q}$ pairs have been produced in the perturbative evolution; these strings thus correspond to the 'preconfinement clusters' in Fig. 2a. The string decays into pieces which are usually forced to correspond directly to final hadrons (including resonances), but in the symmetric Lund model [15] one could equally well have had an intermediate step with 'larger' pieces that would resemble the clusters in the previous model. Thus, the two models are not completely ortogonal, although they are constructed rather differently.

Representing a gluon with a kink, Fig. 3a, means that no additional assumptions and parameters are needed for the gluon fragmentation model, since it is determined by the basic break-up of the colour triplet field as given by quark jets and constrained by, e.g., e^+e^- data. Gluon jet fragmentation is, however, experimentally not well measured and other models can certainly be conceived of. One possibility [16], which can be included in the string framework, is that the gluon stretches a colour octet field which is split into two triplet fields at a junction, Fig. 3b. The position of the junction is determined by the ratio κ_g/κ_q of the string tensions in the octet and triplet fields and if it is larger than two, as suggested by the ratio 9/4 obtained from the Casimir operator magnitudes for the octet and triplet representations of QCD, it is energetically favourable for the octet field to collapse to zero length; thus giving the gluon as a kink on the string. The hadronization of an octet field is, furthermore, unknown and additional assumptions would have to be made to construct a model. On general grounds one would expect an octet field to break by gluon pair creation resulting in the production of glueballs (if existing) and isoscalar particles, but such a model [17] has been found inconsistent with results on η and ϕ production in Υ decays, whereas the Lund gluon-kink model does provide a good description [18].

2.3 Jets at present energies

The importance of the higher order QCD effects included in the parton shower approach has been demontrated by detailed studies of the rate of multijet events, event

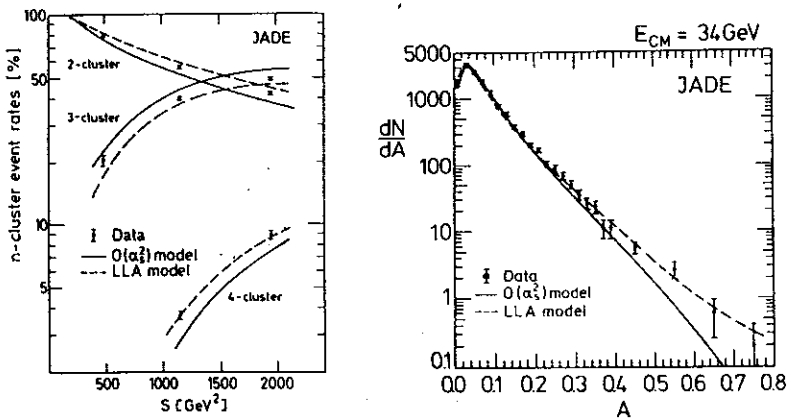

Figure 4: *n-jet event rates versus cms energy and acoplanarity distribution in e^+e^- data compared to model calculations [19].*

shape measures and internal jet properties. Using a cluster algorithm to find jets in e^+e^- annihilation, the JADE collaboration [19] at PETRA observes an excess of 4-jet events as compared to the expectations from order α_s^2 matrix elements. The parton shower model can, however, reproduce the jet rates observed in the data, Fig. 4a, as well as the acoplanarity distribution, Fig. 4b, where the tail of more spherical events is properly generated by the additional gluon radiation compared to the $\mathcal{O}(\alpha_s^2)$ model, which fails in this region. These deficiencies of the $\mathcal{O}(\alpha_s^2)$ model cannot trivialy be cured by an increased α_s since the 3-jet rate will then be overestimated, but the use of an optimized scale choice [20] may improve the agreement [21]. Nevertheless, the higher order effects are still needed for other observables and at higher energies.

The properties of high-$p_\perp$ jets in pp and $p\bar{p}$ collisions are also influenced by parton radiation processes. Thus, the jets measured by the UA1 collaboration [22] show clear evidence for these effects [23] in, e.g., the inclusive fragmentation function

$$D(z) = \frac{1}{N_{jet}} \cdot \frac{dN_{ch}}{dz} \quad ; \quad z = \frac{\bar{p}_{track} \cdot \bar{p}_{jet}}{|\bar{p}_{jet}|^2} \tag{2}$$

of charged particles. This is shown in Fig. 5 together with ISR data from the AFS collaboration [24] for comparison. The reason for the collider jets to be considerably softer is two-fold. Firstly, they are dominated by the intrinsically softer gluon jets, $\approx 60\%$ according to the model, whereas the ISR jet sample contains $\approx 70\%$ quark jets. Secondly, the harder interaction at the collider, resulting in $< p_{\perp jet} > \approx 39$ GeV compared to 13 GeV at the ISR, leads to more parton radiation; an effect which is also more accentuated by the colour octet charge of a gluon jet. The parton radiation also generate significantly enhanced transverse momenta with respect to the jet axis as seen in Fig. 6a. The low-$p_\perp$ part of the distribution depends rather sensitively on the cut applied to remove soft particles from the underlying event as illustrated with the two z-cuts shown for the data. Therefore, a mismatch between data and model calculation for the effective z-cut used may cause the observed difference at low $p_\perp$.

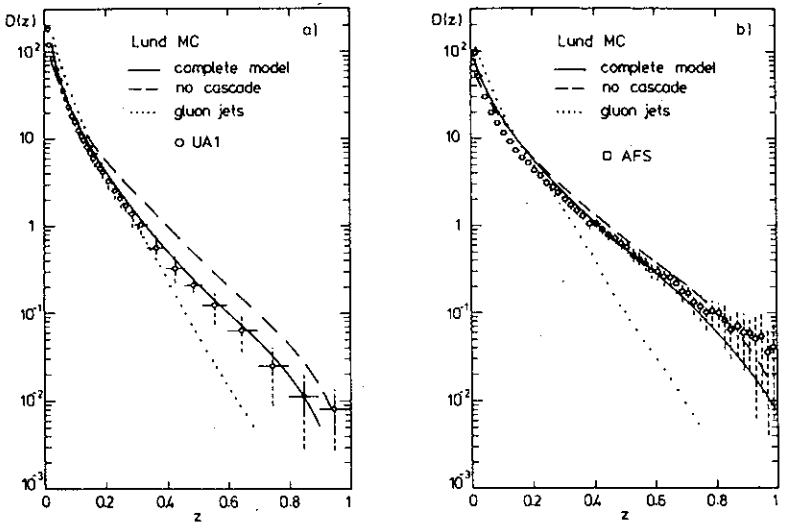

Figure 5: *Fragmentation functions, eq. (2), of high-$p_\perp$ jets at SPS collider (a) and ISR (b) energies. Data from UA1 [22] and AFS [24] collaborations with statistical (full) and systematic (dashed) error bars. The curves represent the model with the parton cascade included (full) and excluded (dashed), with quark and gluon jets mixed according to their relative cross-sections. Pure gluon jets including cascade are also shown (dotted curve) for comparison.*

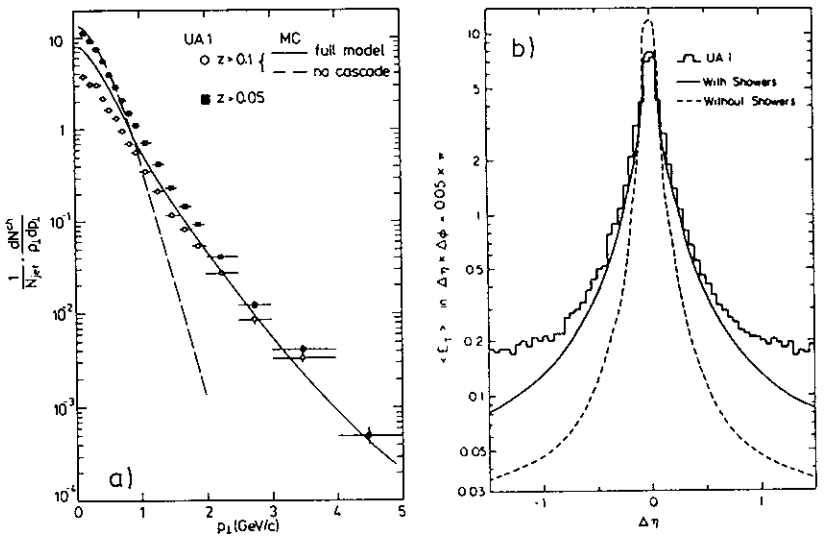

Figure 6: *(a) Transverse momentum distribution of charged particles with respect to the jet axis [23]. (b) Transverse energy flow of high-$p_\perp$ jets versus the rapidity distance to the jet axis [8]. Model curves including (full) and excluding (dashed) parton radiation (in (a) only final state emission).*

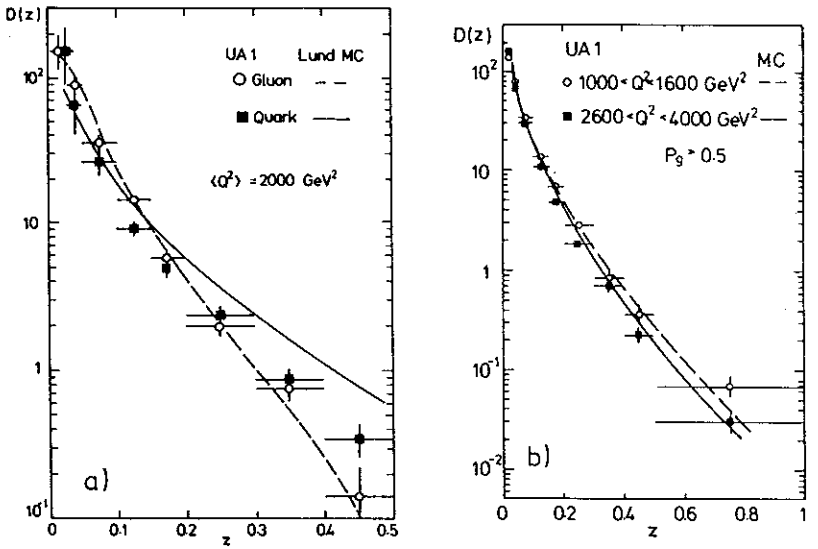

Figure 7: *(a) Fragmentation function for separated quark and gluon jet samples in data compared to pure quark and gluon model predictions. (b) Fragmentation function for gluon enriched jet samples at different Q^2 scales showing scaling violations in data and model.*

The width of a jet, e.g. defined in terms of the energy flow versus rapidity around the jet axis as shown in Fig. 6b, can be rather well described with the inclusion of the final state parton radiation model, whereas without it a much too narrow jet is obtained with non-perturbative fragmentation alone. Although the rapidity distribution away from the jet, $|\eta| \gtrsim 1$, is considerably raised by the initial state parton radiation this is not sufficient to describe the observed energy flow plateau in Fig. 6b. This shows that the underlying event contains more physics than parton shower evolution and simple fragmentation.

In [23] the properties of quark and gluon jets are investigated and a fair agreement between data and model is found. As expected, gluon jets are softer and wider than quark jets, Fig. 7a. There are, however, some tendency of a smaller quark-gluon difference in the data as compared to the model. This could indicate an inadequacy of the model, but since they could also follow from a non-complete separation of quark and gluon jets or other systematic uncertainties in the data the model can be considered satisfactory. The variation with the momentum transfer Q^2 of the longitudinal and transverse jet properties are also found to be essentially the same in data and model, Fig. 7b. In the limited range covered by the UA1 data, the the Q^2 variation is rather small as expected from the dominant leading $\log Q^2$ dependence in QCD.

Current state-of-the-art models for the perturbative jet evolution and the non-perturbative fragmentation, either in terms of strings or clusters, are thus able to reproduce present-day data on jets quite well.

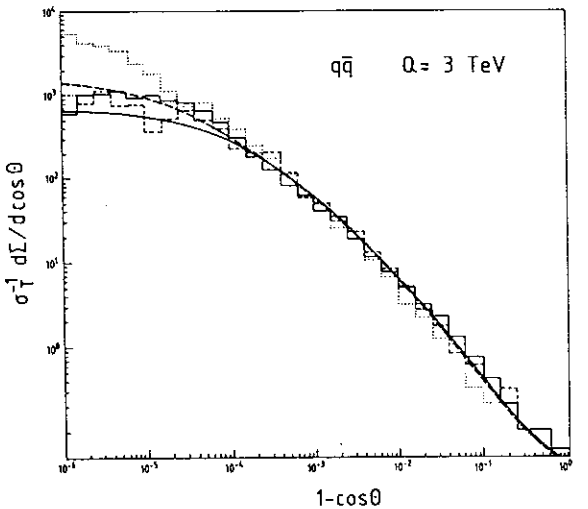

Figure 8: *The energy-energy correlation function, eq. (3), for a quark-antiquark system at $Q = 3$ TeV obtained from Monte Carlo simulation (histograms) of coherent parton shower evolution [4] with $t_{cut} = 0.5$ (full) and 5 GeV^2 (dashed), and without soft gluon interference ($t_{cut} = 5$ GeV^2, dotted) compared to analytical calculations (full and dashed curves) using two separate fits to data of non-perturbative effects [25].*

2.4 Jets at supercolliders

Given that the jet models are based on sound physics input, and not just parametrizations of data, together with their ability to describe present-day jet data it becomes meaningful to make extrapolations to the TeV energy scale that may become available at future colliders; such as LHC, SSC and the ELOISATRON as the most extreme case. There are also theoretical cross-checks that can be made to further increase the confidence in such extrapolations, e.g. by comparing Monte Carlo and analytical calculations in QCD [25]. Such a case is provided by the angular energy-energy correlation function defined by

$$\frac{1}{\sigma}\frac{d\Sigma}{d\cos\theta} = \frac{1}{\sigma}\frac{1}{4}\sum_{A,B}\int_0^1 dx_A dx_B \frac{d\sigma(e^+e^- \to A+B+X)}{dx_A dx_B d\cos\theta}\cdot x_A x_B \qquad (3)$$

where the sum is over all particle pairs A, B with angle θ between $\vec{p}_A$ and the negative of $\vec{p}_B$. This function is shown in Fig. 8 for $e^+e^- \to q\bar{q}$ at an invariant mass of 3 TeV. The peak centered at the back-to-back direction $\theta = 0$ arise from two-jet final states in which one hadron is detected from each jet and the width of the peak is thus a measure of the angular width of a jet and is strongly affected by soft and collinear gluon emission. The two curves correspond to the analytical QCD calculation using two different approximations for the non-perturbative fragmentation based on fits to present data. Since this calculation is based on quite different assumptions and approximations compared to the Monte Carlo, histograms in Fig. 8, it is reassuring

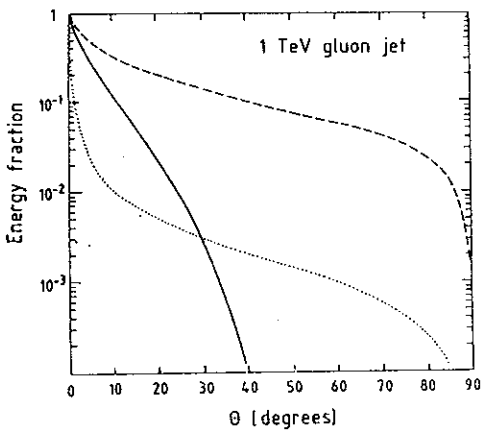

Figure 9: *Energy fraction outside a cone with half-opening angle θ, around the overall jet axis, i.e. parton direction, (dashed curve) and around the reconstructed (sub)jet axes (full curve) obtained from a gluon-gluon system with parton shower at $Q = 2$ TeV and, for comparison, without shower with θ relative to overall jet axis (dotted curve).*

to see the good agreement between the two approaches even when extrapolating to energies much higher than presently available, where they are both tuned to the data. It is also interesting to note that a parton shower algorithm without the coherence among soft gluons taken into account gives a different result compared to the coherent shower and the analytic calculation. This, and other considerations, make the incoherent cascade theoretically disfavoured, although such models can also be tuned to fit most aspects of current data which are, however, in a rather restricted energy region.

Although the bremsstrahlung nature of the QCD radiation predominantly results in soft and collinear parton emission, there will also be occasional hard emission at large angles resulting in the splitting of a jet into a sub-jet structure. Between these two extremes there is, of course, a continous distribution which makes the concept of a jet rather arbitrary from the theoretical point of view. The angular energy flow arising from a 1 TeV gluon jet is illustrated in Fig. 9. A very narrow jet is obtained with pure fragmentation, whereas a significant energy flow also at very large angles (with respect to the gluon direction) arise with the inclusion of parton radiation. The measured jet width will, however, be much smaller and depend on the resolution of sub-jet structures. This illustrates the importance of applying experimentally realistic jet definition criteria to the Monte Carlo generated events when predicting jet properties at TeV colliders. This can be done from the energy flow pattern, e.g., as follows. An idealized 'calorimeter' covers the full azimuthal angle around the beam axis and the pseudo-rapidity region $|\eta| \leq 3$ and is divided into cells of size $\Delta\eta \times \Delta\phi = 0.1 \times 5^0$ in each of which the particle energies of a Monte Carlo generated event are summed. Starting from the cell with largest transverse energy, $E_\perp$, the

transverse energy of nearby cells within

$$\Delta R = \sqrt{\Delta\eta^2 + \Delta\phi^2} \leq 0.7 \tag{4}$$

are summed. If $\sum E_\perp$ exceeds a certain cut-off value, E_c, then all particles/cells within the cone are said to form a jet with axis given by the $E_\perp$-weighted center of the cells. This procedure is iterated until all jets with $E_\perp$ larger than E_c, typically 10–20 GeV, are found. At TeV energies the details of this procedure make no difference. Thus, alternatives like using total energy rather than transverse energy or summing cell 4-vectors obtained from the energy deposited in and the location of the calorimeter cells, give essentially the same results. A coarser grained calorimeter, with cell size $\Delta\eta \times \Delta\phi = 0.2 \times 10^0$, also give similar results. The size of the cone used for the jet definition is, however, important for the jet properties since it regulates not only how many soft, wide angle particles that are included in the jet, but also the experimental resolution to separate nearby jets as indicated above.

In order to give definite predictions of high-$p_\perp$ jet properties at the TeV energy scale [26], we generate events using the Lund PYTHIA program [27] based on the $2 \rightarrow 2$ QCD matrix elements combined with initial and final state parton cascade evolution and followed by hadronization using the Lund string model [13,28]. A cutoff to assure hard scattering is applied by requiring the partons emerging from the simple $2 \rightarrow 2$ process to have

$$x_\perp \equiv \frac{2p_\perp}{\sqrt{s}} \geq 0.1 \tag{5}$$

(Due to the subsequent gluon radiation a final jet with this minimum $p_\perp$ need not emerge.) To illustrate the dependence on centre-of-mass energy results are shown in the following for $p\bar{p}$ collisions at $\sqrt{s}$= 0.63, 2, 18 and 100 TeV, with the $x_\perp$ cutoff corresponding to $p_\perp$ = 30, 100 GeV and 1, 5 TeV, respectively. The events are analysed with the above jet algorithm keeping the parameters fixed with increasing energy, since they correspond to fixed detector properties. The jet multiplicity distributions are given in Fig. 10a and show the increasing number of jets with increasing cms energy. Naturally, most of the increase at TeV energies are 'lower' energy jets, since the cutoff is kept fixed at $E_{\perp jet} > 20$ GeV which can be expected to be enough for the jets to stand out clearly above the underlying event. Seen on a TeV energy scale, however, the events are often quite clean with only a few, narrow energy clusters surrounded by additional activity at a reduced energy, Fig. 10b. Of course, the number of jets depend rather strongly on the basic jet resolution as illustrated in Fig. 10a by the curve for $\Delta R = 0.2$, which is about the smallest value possible for the given calorimeter granularity before fluctuations become important when only a few cells are used to define a jet.

The characteristics of 'typical high energy' jets at each centre-of-mass energy is extracted by only taking jets in a 'window' around $x_\perp \simeq 0.1$ and separating quark and gluon jets [26]. The longitudinal distribution within the jets is illustrated in Fig. 11a by the fraction of jet energy carried by particles with a minimum fractional energy $z = E_{particle}/E_{jet}$, i.e. the integral of the energy-weighted fragmentation function

$$I(z) = \int_z^1 dz'\, z' \cdot D^{all}(z')\,, \quad D^{all}(z) = \frac{1}{N_{jets}} \cdot \frac{dN^{all}}{dz} \tag{6}$$

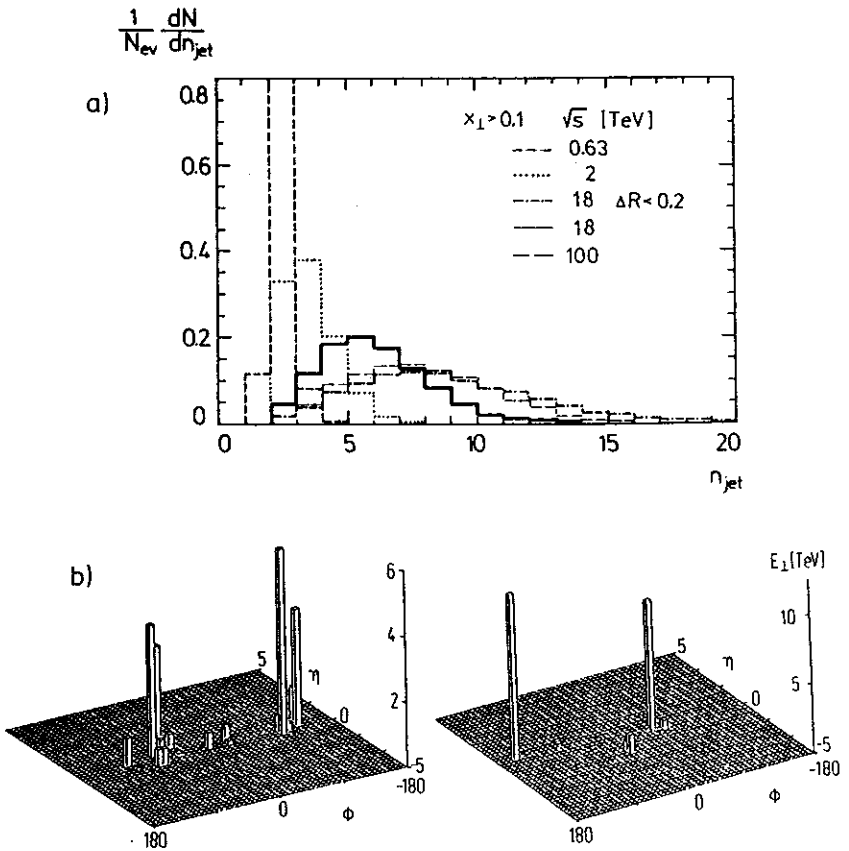

Figure 10: *(a) Jet multiplicity in hadron collider high-$p_\perp$ events. Standard jet cone size $\Delta R = 0.7$ in all cases except the one marked.*
(b) Transverse energy distribution in the pseudorapidity-azimuthal angle space for two Monte Carlo events at $\sqrt{s} = 100$ TeV with a hard $2 \to 2$ QCD scattering with $p_\perp > 10$ TeV.

The much softer nature of the gluon jets compared to quark jets is evident as is the increased softness (in the scaling variable) for higher energy jets; e.g. 10% of the quark jet energy is carried by particles with $z > 0.45$, 0.3 at $\sqrt{s} = 0.63$, 100 TeV corresponding to particle energies of ~ 15, 1500 GeV. The decreasing width of a jet with increasing energy is shown in Fig. 11b in terms of the integrated energy flow inside a cone with half-angle θ around the jet axis; e.g. 90% of the quark jet energy is inside a cone of 18^0, 9^0 for a quark jet of 30 GeV and 5 TeV, respectively. The particle flow is less collimated compared to the energy flow due the occurence of lower energy particles at wider angles [26].

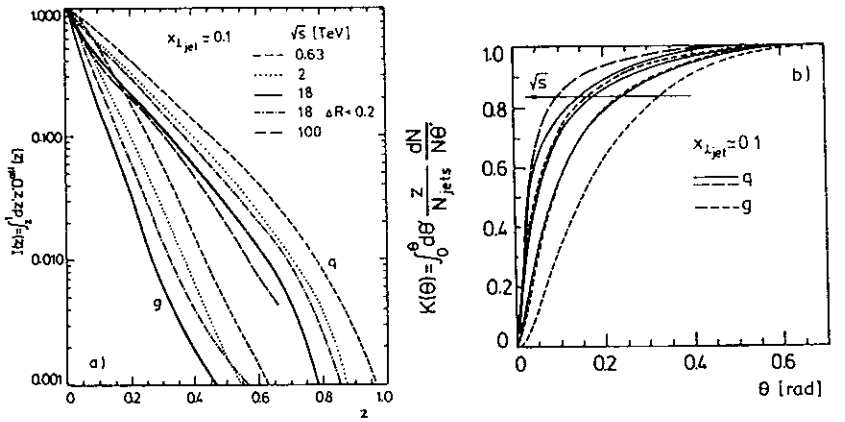

Figure 11: *Fraction of jet energy (a) carried by particles with fractional jet energy larger than z, and (b) within a cone of half-angle θ around the jet axis; for quark (q) and gluon (g) jets with $x_\perp \simeq 0.1$ at different cms energies of $p\bar{p}$ collisions. In (b), the curves are for cms energies of 630 GeV, 2, 18 and 100 TeV, respectively, when going towards $\theta = 0$.*

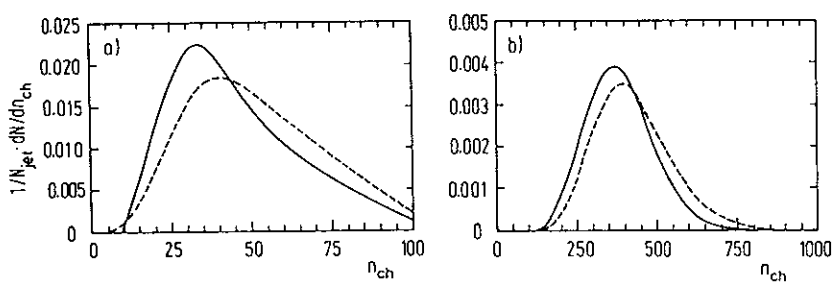

Figure 12: *(a) Charged particle multiplicity for jets with $E_\perp \approx 5$ TeV (full) and 15 TeV (dashed). (b) Total charged particle multiplicity in events with a QCD $2 \to 2$ hard scattering with $p_\perp > 10$ TeV, for two somewhat different models of the underlying event.*

The expected charged particle multiplicity in high-$p_\perp$ jets and in total for high-$p_\perp$ events at the ELOISATRON is shown in Fig. 12. The total multiplicity in particular, but also the jet multiplicity, should only be taken as an indication since they depend on the model used for the underlying event. As mentioned above, see Fig. 6b, the underlying event in high-$p_\perp$ events is not well understood making extrapolations rather uncertain. This is related to the absence of a proper understanding of the spectator partons and minimum bias event properties in general.

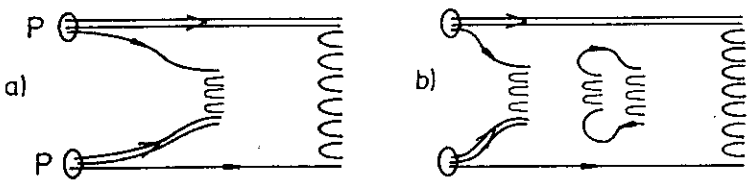

Figure 13: *Low-$p_\perp$ proton-proton interaction in the DTU model. (a) The simplest case giving two quark-diquark strings, hadronizing independently of each other. (b) Next order correction with sea quark interactions giving two additional quark-antiquark strings.*

3 Minimum bias physics and beam jets

The low-$p_\perp$ interactions of minimum bias events provide most of the inelastic hadron scattering cross-section and in that sense constitute the dominant soft interaction. Although high statistics data on very detailed properties of the final multiparticle state are available our understanding of the interaction mechanism is far from being understood. The hadronization models discussed, which successfully describe e^+e^- annihilation, deep inelastic scattering and the high-$p_\perp$ jets in hadron scattering, could in principle work also for low-$p_\perp$ interactions. The problem is that we have no calculable underlying parton level process which can define the structure of the colour fields to which the fragmentation models can be applied. Nevertheless, models to describe the production of the final hadron state in minimum bias events have been developed and some of them work rather well in describing the data.

3.1 Minimum bias models

The simplest model is provided by the 'old' Lund low-$p_\perp$ model [29] where it is assumed that the main features can be understood by the fragmentation of a single colour triplet field, which hadronizes similar to the one in e^+e^-. Thus, a string is stretched between the interacting hadrons with the valence quarks distributed along it according to a phenomenological recipe. It is remarkable how well this simple model can be tuned to fit data concerning the beam and target fragmentation regions at fixed target energies [30], but with increasing energy the model fails badly with too little activity in the central region and is therefore not useful at collider energies.

Another approach is given by the dual topological unitarization (DTU) scheme [31], which is based on Regge theory, with 'cut pomerons', to give the probablity for a certain number of strings to be formed as illustrated in Fig. 13. In the lowest order process, a quark from one beam proton is connected with a diquark from the other and the remaining diquark with the corresponding quark, thus forming two colour triplet fields. Higher order effects give additional strings between sea quarks and antiquarks from the interacting protons. Quark structure functions are used to assign momenta to the quarks, antiquarks and diquarks, thereby specifying the invariant masses of the strings, which can then be hadronized using normal models

from e^+e^- annihilation. This provides a non-perturbative approach to multiparton interactions giving a rather well defined model which is in fact very successfull in reproducing data even up to the SPS collider energy with respect to multiplicities, central rapidity plateau, long range correlations and $p_\perp$ increase with multiplicity [31]. Some of these observables were, however, not predicted by the model, but reproduced by tuning and adding new detailed ingredients to the model. There may also be problems of a more fundamental kind. Firstly, the model is founded on Regge theory and one may question whether this is the proper soft limit of QCD. Secondly, there are no dynamical gluons in the model. This is in my view disturbing since we know that in perturbative QCD, gluon scattering become dominating as the momentum transfer is decreased. Based on the assumption of a smooth transition to the soft limit one might therefore expect the gluons to play an important dynamical role in minimum bias interactions. Also the connection to diffractive scattering, although covered by Regge theory, may be problematic if the exchanged pomeron is a gluonic object as discussed below. Although this model works effectively in describing many aspects of the data, it need not reveal the true interaction mechanism. In any case, alternative models are important tools to investigate other ideas of the interaction mechanism.

A new approach based on multiparton scattering in perturbative QCD has recently been developed [32,33], which leads to a natural connection to high-$p_\perp$ scattering. The starting point is the cross-section in leading order QCD

$$\sigma(p_\perp) = \int_{p_{\perp min}} dx_1 dx_2 di \sum_{i,j} f_i(x_1, Q^2)\, f_j(x_2, Q^2)\, \frac{d\sigma}{di} \qquad (7)$$

which increases strongly for decreasing $p_{\perp min}$ and in fact becomes equal to the total cross-section at the SPS collider for $p_{\perp min} \simeq 1.5$ GeV. This is not necessarily unphysical since this cross-section is not the proton-proton cross-section, but a parton-parton one. Viewing the proton as a beam of partons one can interpret the ratio $\sigma(p_{\perp min})/\sigma_{tot}$ as the number of parton-parton scatterings per proton-proton collision. Thus, a multiparton scattering situation naturally arise. One may still worry whether a perturbative calculation is really applicable at such small momentum transfers, but this is not a conceptual problem but rather a technical one. In particular, higher order QCD corrections may be large making the numerical results unreliable.

In a first attempt this probability for multiple parton scatterings, using a fixed value of $p_{\perp min}$, was introduced in the Lund hadron scattering Monte Carlo [32]. The additional scatterings have the effect of producing a more complicated string topology with either extra strings or more kinks on the existing ones, which in turn lead to an increased hadron multiplicity. In comparison to observed minimum bias event multiplicities, Fig. 14a, the result is not satisfactory, but encouraging when compared to the result of the previous case, including single $2 \rightarrow 2$ hard QCD processes and initial plus final state parton cascade evolution as discussed above. The result is, however, very sensitive to the exact value of the new basic parameter $p_{\perp min}$, as seen in Fig. 14a. In an improved version of the model an impact parameter picture is introduced [33]. For a large overlap between the colliding hadrons, associated with a small impact parameter, an enhanced probability for multiple interactions occur, resulting in 'more strings' and consequently increased multiplicity. An event with a high-$p_\perp$ process, i.e. a manifest parton-parton scattering, should then involve a

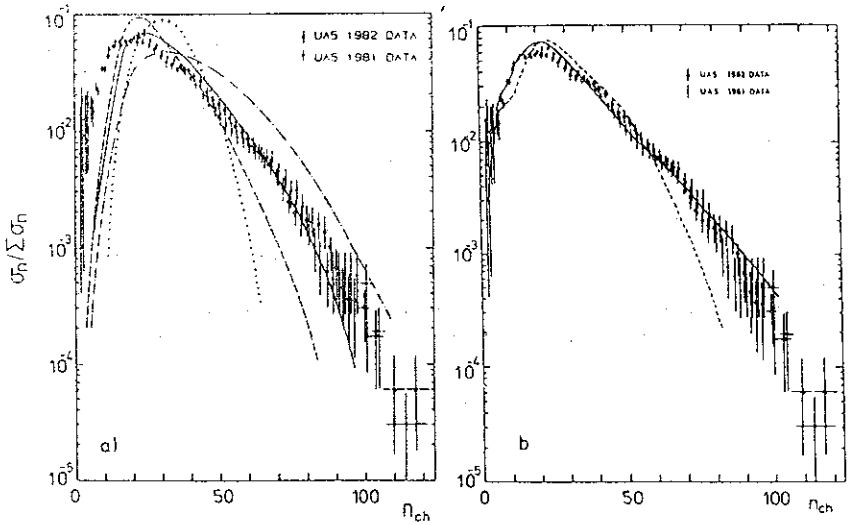

Figure 14: *Charged particle multiplicity distribution in 540 GeV $p\bar{p}$ collisions [34] in comparison to models. (a) Simple multiparton scattering model with cutoff $p_{\perp min}$ = 2 GeV (dashed), 1.6 GeV (full) and 1.2 GeV (dash-dotted); excluding multiple scattering (dotted). (b) Multiparton scattering in an impact parameter model with varying (full) and fixed (dashed) impact parameter. In all cases hard scattering processes with initial and final state parton radiation is included. From [33].*

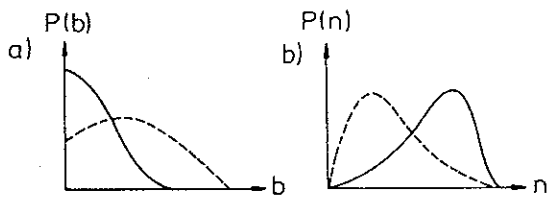

Figure 15: *Probability distributions for (a) impact parameter and (b) multiplicity in minimum bias events (dashed) and high-$p_\perp$ events (full).*

larger overlap, compared to the average minimum bias event, and therefore give rise to a larger multiplicity, Fig. 15.

To construct this model in detail the distribution of matter in the colliding hadrons has to be specified and a few simple functions was considered to describe the effective parton distributions. A solid sphere, a Gaussian or an exponential distribution give similar results that are not able to properly describe the pedestal effect, i.e. the increased rapidity plateau in high-$p_\perp$ jet events. A better result is obtained with a

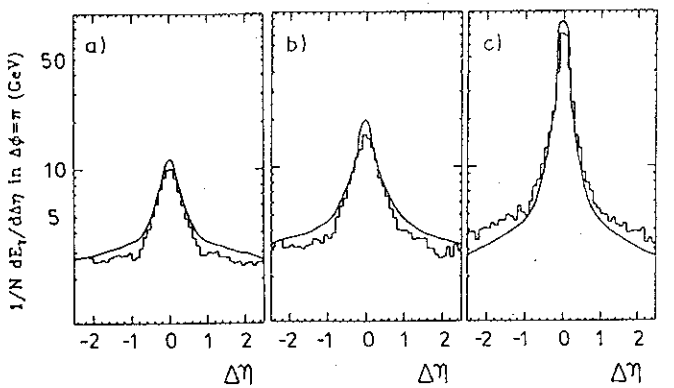

Figure 16: *Jet energy profiles in rapidity ($\Delta\eta = \eta - \eta_{jet}$) in the 'same side' region, $|\phi - \phi_{jet}| < 90^0$. UA1 data [35] in comparison to multiparton scattering model [33] for (a) $E_{\perp jet} > 5$ GeV, (b) $E_{\perp jet} > 10$ GeV and (c) $E_{\perp jet} > 30$ GeV.*

double Gaussian of the form

$$\rho(r) = \frac{1-\beta}{a_1^3} e^{-r^2/a_1^2} + \frac{\beta}{a_2^3} e^{-r^2/a_2^2} \qquad (8)$$

corresponding to a small core of radius a_2 with a fraction β of the matter in the hadron, which has radius a_1. One may speculate whether this two-component structure is related to the pion cloud or a simple representation of a more complicated structure, e.g. with three cores corresponding to the valence quarks. Numerically, $\beta = 0.5$ and $a_1/a_2 = 5$ was found appropriate. The problem remains with the divergence for $p_\perp \to 0$ of the QCD $2 \to 2$ matrix elements, which are used for calculating the multiparton interaction probability. A regularization was enforced by replacing the $1/p_\perp^4$ dependence with $1/(p_\perp^2 + p_{\perp 0}^2)^2$ in the matrix element and using $\alpha_s(p_\perp^2 + p_{\perp 0}^2)$, such that the basic cut-off parameter is $p_{\perp 0}$ which is assigned the value 2 GeV in order that the model can reproduce the collider multiplicity distribution, Fig. 14b, rather well. The increasing rapidity plateau with energy can be reproduced and its behavoiur in high-$p_\perp$ events is better described, although the agreement is not perfect, see Fig. 16. Correlations in forward-backward multiplicity and $p_\perp$-multiplicity gets a natural explanation in terms of increased 'activity' from additional parton scatterings [33].

This model is thus able to give a rather satisfactory description of basic observations of soft interactions. The smooth connection to hard scattering processes throught its modern parton language basis is theoretically appealing. This may, however, also be a weakness in the sense that such a description may be inadequate, or even invalid, at small momentum transfers. In any case, calculational problems are certainly present in terms of possibly large higher order corrections in the perturbative expansion and a rather strong dependence on the basic $p_\perp$ cutoff. Although this cutoff is introduced in a technically different way by the parameters $p_{\perp min}$ and $p_{\perp 0}$ in the simple model and the impact parameter model, respectively, they represent the same problem giving rise to a similar kind of uncertainty. Additional uncertainties

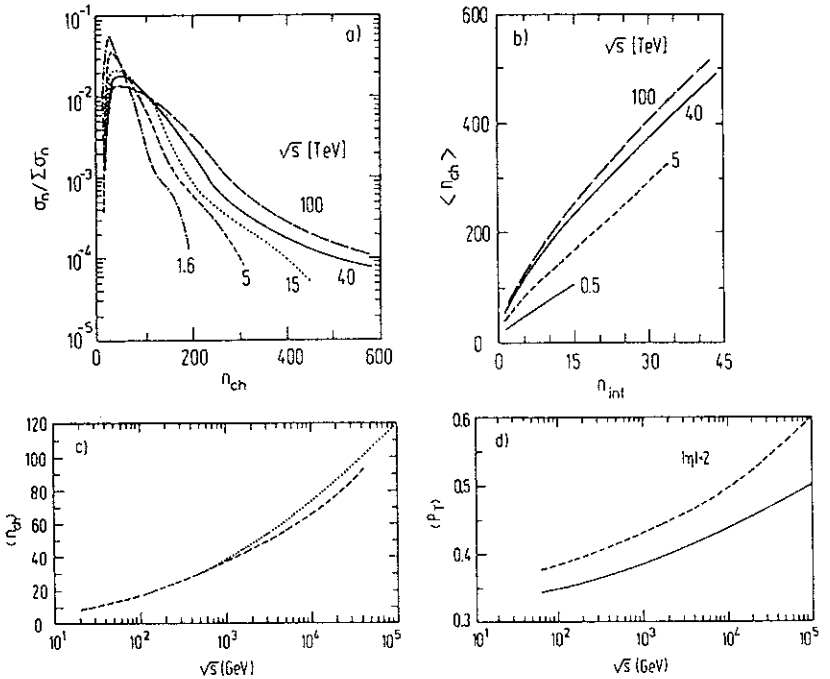

Figure 17: *Expectations for $p\bar{p}$ collisions at TeV energies based on the model including impact parameter dependent multiparton scatterings and high-$p_\perp$ processes with parton cascade evolution. (a) Charged particle multiplicity distribution. (b) Dependence of mean charged multiplicity on the number of parton-parton interactions. (c) Energy dependence of mean charged multiplicity for a fixed $p_{\perp 0}$ = 2 GeV (dotted) and $p_{\perp 0} = 2 + 0.08\, ln(\sqrt{s}/540)$ (dashed). (d) Energy dependence of mean transverse momentum of central (dashed) and all particles (full).*

arise through the choice of string configurations which is not quite clear in case of multiple interactions. Nevertheless, we use this new interesting model for extrapolations to higher energies, but stress that the results should not be taken too literally but rather as an educated guess of what can be expected at TeV colliders. In particular, an unknown energy dependence of the $p_{\perp 0}$ parameter cannot be excluded, although it can be argued to be essentially a constant or only varying logarithmically with energy.

The multiplicity distribution, Fig. 17a, develops a very long tail with increasing energy. This arises through events having many parton-parton collisions, Fig. 17b, producing additional strings and 'longer' strings with gluon kinks. The dependence of the mean multiplicity with energy is given in Fig. 17c, for a fixed regularization $p_{\perp 0}$ = 2 GeV and for a mildly energy dependent one, but a stronger variation is not excluded. The increasing number of parton collisions with increasing energy also give rise to an increased transverse activity as illustrated by the mean $p_\perp$ in Fig. 17d; in particular the central rapidity region is affected.

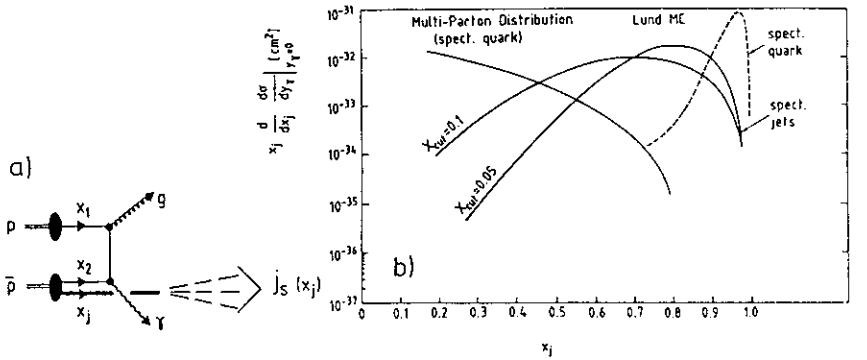

Figure 18: *(a) Example of process for the study of correlations between the hard scattering and the spectator jet. (b) Momentum distribution of the spectator jet in the Lund approach and using multiparton momentum distributions, see text.*

3.2 Beam jets in high-$p_\perp$ processes

The properties of the underlying event in hard scattering processes is given by the remaining partons in the colliding hadrons. These are often considered to be spectators that do not experience any hard scatter. Nevertheless, they provide the dynamics for generating the colour field structure of the underlying event, which is in the Lund model connected to the high-$p_\perp$ partons. It is natural to relate the problem of the underlying event to that of minimum bias event structure and thus try to solve both with the same model.

The properties of beam jets in high-$p_\perp$ events has hardly been investigated experimentally; in particular the correlations with the high-$p_\perp$ process would be interesting. In a first study [36] the consequences of two simple and orthogonal models were considered for the process $p\bar{p} \to \gamma g + j_s + X$ in Fig. 18a. The distribution of scaled momentum, x_j, of the spectator jet is shown in Fig. 18b, for a prompt photon with $p_\perp$ > 10 GeV at zero rapidity. In one model, used in the previous Lund Monte Carlo [37], all spectator partons are assumed to act as a single colour charge with momentum fraction $x_s = 1 - x_2$, reflecting the hard scattering directly, and stretching a single string which hadronizes in the usual way. A hard spectator jet will thus arise, the exact distribution depending on the detailed definition of the jet concept. A completely different, much softer, spectrum is obtained in a model using 2-parton momentum distributions $V(x_2, x_j)$ to admit that the remaining energy is distributed on different spectator partons that hadronize independently. The division into several spectators in the latter model may seem unphysical but illustrates the main point, i.e. whether the spectator can be considered as a whole or not which is not obvious as will become clear in the following.

To illustrate the large uncertainties concerning the beam jets we use the various options available in the Lund hadron scattering Monte Carlo [27]. Fig. 19 show the angular energy flow, $x_E/\sigma \cdot d\sigma/d\log\theta$, of the final hadrons, with $x_E = 2E_h/\sqrt{s}$, in $p\bar{p}$ collisions at $\sqrt{s}$= 100 TeV having a hard $2 \to 2$ QCD scattering with $p_\perp$ > 10

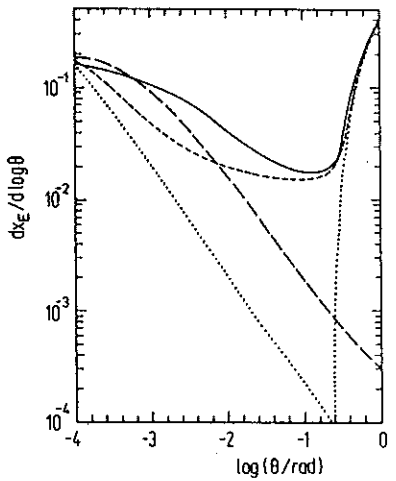

Figure 19: *Scaled angular energy flow with respect to the beam axis in $p\bar{p}$ collisions at $\sqrt{s}$= 100 TeV having a hard $2 \to 2$ QCD scattering with $p_\perp > 10$ TeV. The curves are for simple process (dotted), including parton radiation in initial (and final) state (dashed) and, in addition, multiparton scatterings (full). Result for minimum bias model, based on multiple scatterings, is included for comparison (long-dashed).*

TeV. Although the transverse partons and the forward spectator partons are usually connected by a string, the final jets are very clearly separated in the simplest model, but less so when the initial state parton radiation is taken into account. This produces a wider energy flow in the beam jet, which is also strongly increased by the multiparton scattering mechanism. Even if the parton radiation process can be considered as rather well controlled, the multiple scattering model introduces significant uncertainties of the beam jet properties. For comparison, the result of the minimum bias model is also given. Concentrating on the beam jet by selecting a forward cone of 100 mrad half-angle, the longitudinal and transverse particle spectra are shown in Fig. 20. For high-$p_\perp$ events the rapidity distribution is strongly influenced by the gluon radiation and also to some extent by multiparton scattering. The transverse momentum distribution is similarly influenced, although the large-$p_\perp$ tail is totally dominated by the parton cascade effects. The multiplicity distribution is particularly sensitive to the inclusion of these effects, Fig. 21, and the predictions correspondingly uncertain.

In summary it is evident that the beam jet properties are strongly dependent on variations within the model. This is not particular for this model, but other models would tend to add to the 'theoretical' uncertainty and the predictions for TeV energies will therefore span a rather wide region. It would be very valuable to have data from the present colliders to constrain the models, or even rule some out, in order to obtain a better understanding of the interaction mechanisms and be able to make more solid predictions to be tested at higher energies.

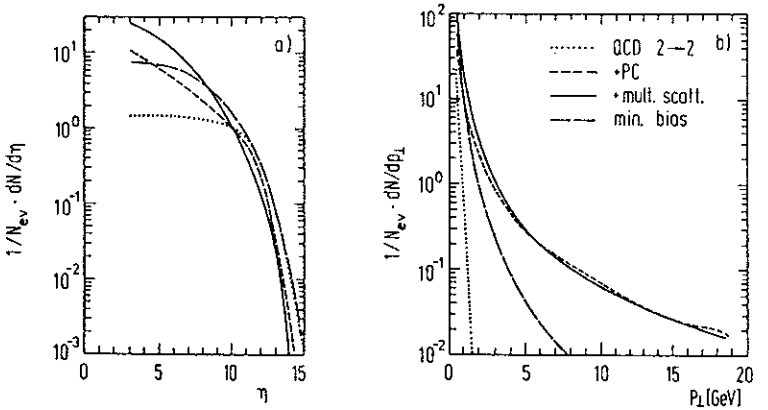

Figure 20: *Distribution in (a) pseudorapidity and (b) transverse momentum of charged particles in a forward cone of 100 mrad half-angle to the beam axis of $p\bar{p}$ collisions at $\sqrt{s}$= 100 TeV having a hard $2 \to 2$ QCD scattering with $p_\perp > 10$ TeV. Model curves as in Fig. 19.*

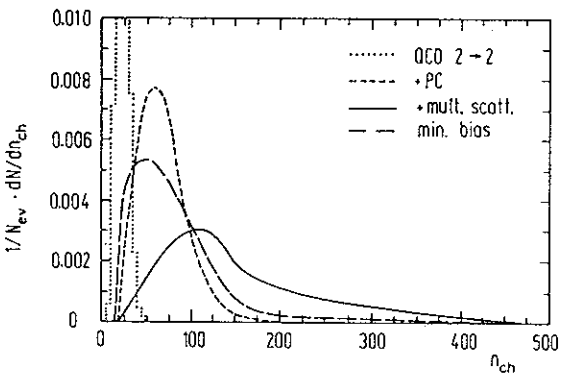

Figure 21: *Beam jet charged particle multiplicity distribution under the same conditions as in Fig. 20.*

3.3 Speculative discussion

Given the lack of a fundamental understanding of soft interaction mechanisms one has to consider modifications of the discussed models and, of course, be open to completely new ideas. The hadron remnant in a high-$p_\perp$ interaction has conventionally been treated as a genuine spectator, i.e. non-interacting and more or less as a single system, Fig. 22a. Some of the remnant partons may, however, interact via additional essentially independent scatterings as in the multiparton scattering model and other interaction mechanisms are also possible. Given the additional gluon radiation in

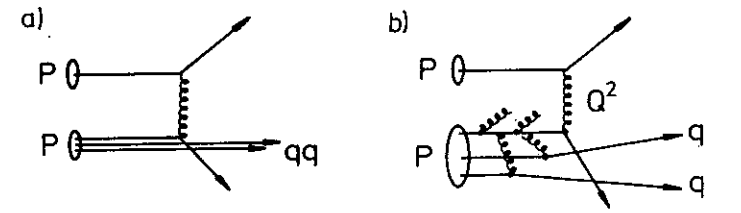

Figure 22: *Illustration of (a) 'true' spectator and (b) 'interacting spectator'.*

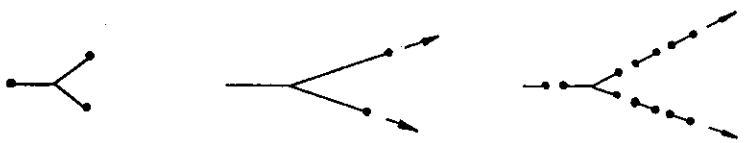

Figure 23: *Stretching of a Y-shaped baryon string due to a hard scattering and additional spectator interactions resulting in a non-leading baryon.*

the process, gluon exchanges like in Fig. 22b may occur giving rise to 'interacting spectators' which are connected to the large Q^2 process. This would be a kind of higher twist effect, but there are certainly severe calculational problems, such as what structure functions and q^2 scale to use and how to obtain the colour field structure in order to apply a hadronization model, but the qualitative effects are clear. With increasing Q^2 one would expect the forward jet to become softer and wider. The leading baryon may furthermore disappear, namely as illustrated in Fig. 23 where the baryon is considered as a Y-shaped string and the remaining valence quarks are separated through this additional gluon exchange giving rise to leading mesons before the baryon is formed. In $p\bar{p}$ collisions the baryons may totally disappear, but only if separate strings are formed between the valence quarks and antiquarks which is presumably very unlikely.

More generally one may consider whether separate strings formed in a collision can interact with each other if they are 'overlapping' in space-time. In particular with multiple interactions, in the DTU model or the pertubative QCD approach, such cases arise. The degree of overlap depends on the transverse size of such colour flux tubes, which is usually taken as a typical hadron diameter of $\sim$ 1 fm. Also very important is, however, the internal field configuration. One possibility [38] is a thin core surrounded by a more extended field, similar to a vortex line in a type II superconductor. In this case the most essential properties are given by the thin core, e.g. the dynamics via the massless relativistic string, and the effective overlap for interactions between strings would be reduced and the assumption on non-interacting strings be better founded.

The possibility remain, however, that overlapping strings interact and could coalesce into a field of higher colour representation. Alternatively, the original interaction, e.g. via multiple gluon exchange, can generate higher colour charges on the separating hadron remnants leading to a colour field of a higher rank in between them. The probability for the generation of such different fields is unclear, but a

model based on a random walk in colour space has been proposed for the case of relativistic heavy ion collisions [39]. A model based on gluon exchange dynamics in QCD would be even more interesting. The most important question is, however, whether higher rank fields are more likely to be produced with increasing centre-of-mass energy? The string constant κ, i.e. energy per unit length, of such fields can presumably be larger through the advocated connection to the magnitude of the Casimir operator which increases for higher colour representations. The increase is, however, not very strong as shown in Table 1 for the next few higher representation of the SU(3) colour group in comparison to the basic triplet field. In the Lund model the string breaking is treated as a tunneling process giving a quark production probability

$$P \sim e^{-\frac{\pi}{\kappa}m_q^2}\, e^{-\frac{\pi}{\kappa}p_\perp^2} \tag{9}$$

which is Gaussian in quark mass and transverse momentum. A simple application to higher rank fields would thus give an indication of the dependence on the string constant, κ, as illustrated in Table 1. A moderate increase in mean transverse momentum, $< p_\perp > \sim \sqrt{\kappa}$, can thus be be expected and a significant increase of strangeness production. Charm production, which is normally absent, may be dramatically increased to an observable level.

Table 1

rank of field	3	$6,\bar{6}$	8	$10,\overline{10}$	15	15′
κ/κ_3	1	10/4	9/4	9/2	4	7
$< p_\perp >$ (GeV)	0.4	0.64	0.6	0.84	0.8	1.0
$s\bar{s}/u\bar{u}$	0.3	0.6	0.6	0.77	0.74	0.84
$c\bar{c}/u\bar{u}$	10^{-11}	$4\cdot10^{-5}$	10^{-5}	$4\cdot10^{-3}$	$2\cdot10^{-3}$	$3\cdot10^{-2}$

A major problem is, however, that the decay or hadronization of such a field is not known. Given the fundamental colour charges 3, $\bar{3}$ and 8 of quarks, antiquarks and gluons the screening of the field in the breaking process would have to proceed by pair production of composite parton states, e.g. a 15-plet field could be broken by $qg - \bar{q}g$ pair production. Alternatively, $q\bar{q}$ and/or gluon pair production can be made in a stepwise manner that successively reduce the rank of the intermediate field. Thus, the fragmentation function of such fields is basically unknown, but the larger energy per unit length implies a concentration of the energy and presumably a correspondingly higher central rapidity plateau. Correlations of forward-backward multiplicities and $p_\perp$-multiplicity would arise naturally through the occurence of different event classes in terms of different fields.

Although these speculations are not very quantitative they illustrate the fact that confinement is an unsolved problem and completely different approaches are certainly possible. One such is based on hydrodynamical concepts applied to a quark-gluon plasma [40], but is not yet developed to the extent that definite predictions for TeV colliders can be made.

4 Pomeron structure and diffractive scattering

The differential cross-section for elastic and diffractive scattering of hadrons has been well measured by the detection of the (quasi-)elastically scattered particle and can

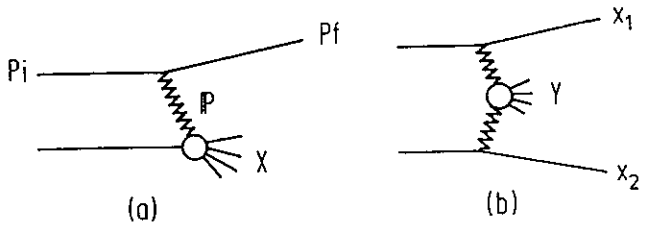

Figure 24: *(a) Pomeron exchange in single diffractive scattering. (b) Double pomeron exchange process.*

be 'understood' in Regge theory in terms of pomeron exchange [41]. Unfortunately, this has not lead to any real understanding of the true nature of the pomeron and its interactions. Since they involve hadrons and have cross-sections of order millibarn, they are clearly strong interaction processes. It is therefore natural to ask whether they can be understood in a 'modern language' based on an underlying parton level process. In particular, the pomeron itself may have a parton substructure, perhaps mainly of a gluonic nature [42].

In the following we will concentrate on the single diffraction process

$$h_1 + h_2 \to h_1 + X, \tag{10}$$

with one beam hadron quasi-elastically scattered with a remaining large momentum, $x = p_f/p_i > 0.9$, and the other excited to a system X (Fig. 24a). This process has been studied with various combinations of incident particles and at different energies. Even up to the highest available SPS collider energies [43], it shows a consistent behaviour of the cross-section in terms of the excitation mass, M_X, and momentum transfer, t, to the system X. However, the X system itself has not been much studied and its properties are largely unknown. The mass and rapidity of the excited system is given by

$$M_X^2 = (1-x)s\ , \quad y = \ln\frac{\sqrt{s}}{M_X} = \ln\frac{1}{\sqrt{1-x}}\ \ (= 1.5\ \ for\ \ x = 0.95) \tag{11}$$

such that very large masses can be excited in a rather central region at TeV colliders, Table 2. Double pomeron exchange, Fig. 24b, provide pomeron-pomeron collisions giving excited states of mass

$$M_Y^2 = (1-x_1)(1-x_2)s \tag{12}$$

that can also be quite substantial at future colliders. The study of these systems should provide important information about the pomeron, its possible structure and interaction mechanisms which are essentially unknown at present.

Table 2

	M_X	$(x = 0.95)$	M_Y	$(x_1 = x_2 = 0.95)$
ISR	13	GeV	3	GeV
$Sp\bar{p}S$	140	GeV	30	GeV
LHC	4	TeV	0.9	TeV
ELOISATRON $\sqrt{s} = 100$ TeV	22	TeV	5	TeV

4.1 Models for the pomeron-proton interaction

Based on the observation that factorisation (between the upper and lower vertices in Fig. 24a) holds to a good approximation, the system X can be said to be the outcome of a pomeron-proton interaction. The nature of this interaction will clearly influence the properties of the diffractive system, e.g. whether its overall shape is isotropic in its centre-of-mass or longitudinal along some prefered axis. At high enough mass M_X, high-$p_\perp$ jets may even emerge [44] to signal the occurence of a hard scattering at the parton level!

A coherent pomeron-proton interaction could conceivably excite the proton wave function as a whole without any prefered direction. This could lead to a decay into a spherically symmetric state, if angular momentum effects are not important. Even for a system which is overall isotropic there can be internal asymmetries. The momentum vector of the final baryon may, for example, be aligned with the direction of the incoming proton. A mechanism for this is not easily constructed within a fireball type model, but one could perhaps think of 'hard' valence quarks which go forward with less disturbance, whereas the softer sea and glue components 'thermalize' with the many soft gluons that could make up the pomeron.

A very interesting model [45] for the pomeron interaction is based on the apparent similarity with photon interactions, which is deeper than the obvious diagrammatic one (in Fig. 24a replace the upper proton line with a lepton and the exchanged pomeron with a photon). The pomeron is thus assumed to have a pointlike coupling to quarks with a strength, β, that can be determined from elastic scattering. Within this framework the differential cross-section for single diffraction can be written as (when the approximation $\alpha_P(t)$=1 is made for simplicity) [45]

$$\frac{d^2\sigma}{dtdM_X^2} = \frac{1}{4\pi}[3\beta F_1(t)]^2\frac{1}{M_X^2}(1-\frac{M_X^2}{s})\beta^2\tilde{F}_2(x,Q^2) \tag{13}$$

where F_1 is the proton formfactor (upper vertex in Fig. 24a) and $\tilde{F}_2$ the (lower vertex) proton structure function (normal F_2 but without quark charges) evaluated at $x = \frac{Q^2}{M_X^2+Q^2} \approx \frac{Q^2}{M_X^2}$ and $Q^2 = -t$. The resemblence with deep inelastic scattering appears clearly in the cross-section formula, which for deep inelastic electron or muon scattering is

$$\frac{d^2\sigma}{dQ^2dM_X^2} \approx \frac{1}{4\pi}[\frac{e^2}{Q^2}]^2\frac{1}{M_X^2}(1-\frac{M_X^2}{s})F_2(x,Q^2) \tag{14}$$

in the kinematic region ($y \ll 1$, $|Q^2 - m_p^2| \ll M_X^2$) of interest for the comparison with single diffractive scattering.

The amazing thing with eq. (13) is that it has no free parameters and yet it does reproduce data quite nicely [45]. Furthermore, this model has very clear consequences for the properties of the system X. Viewed in the pomeron-proton cms, a proton quark (or antiquark) would be back-scattered by the pomeron, leaving forward-going spectator quarks (in the simplest case a diquark). The separated colour charges are then expected to stretch a colour field which hadronize in the same way as is obseved in deep inelastic scattering. Obviously, this leads to a longitudinal event structure with a leading baryon in the direction of the initial proton. Based on the pomeron-photon analogy one can thus construct a detailed model for the production of the

diffractive system [46]. It is still unclear, however, why the pomeron should couple in a pointlike way, or perhaps only effectively appears to. Furthermore, why should it couple to quarks only and not to the gluon component of the proton?

In another approach the pomeron is considered to have hadronic properties and gluonic interactions could then be of great importance. Being a strongly interacting object, one could expect the pomeron to contain coloured parton constituents. In such a pomeron-hadron analogy the pomeron-proton interaction should resemble a normal hadron-hadron interaction and typically give rise to a minimum bias topology, i.e. longitudinal event shape with a leading baryon effect. It was suggested more than ten years ago that the pomeron could be a gluonic system [42]. However, the simplest case of a two-gluon system, where the two gluons could couple to the same or different quarks, has theoretical problems with gauge invariance and factorization breaking [47]. A more complicated many-gluon system may work, but is difficult to calculate and is still an open question. Some non-perturbative developments have, however, been made recently [48] in this context.

Experimentally there has been progress by the clear observation of a longitudinal structure of the X system (in its cms) both at ISR [46] and the SPS collider [49]. Although the diffractive mass is only a few GeV at the ISR, a detailed comparison with model simulations show a clear longitudinal structure along the pomeron-proton collision axis. The final state proton momentum is, furthermore, found to be aligned along the incoming proton, an effect which becomes more pronounced with increasing diffractive mass [46]. At collider energies, the longitudinal structure is directly revealed in the rapidity distribution of the hadrons in the diffractive system [49]. Spherical symmetry is thus clearly ruled out and thereby all kinds of 'fireball' models. A further interesting result is the evidence for pomeron single-quark interactions obtained by a study of the fully reconstructed exclusive diffractive reactions $pp \to (\Lambda^0\phi^0K^+)p$ and $pp \to (\Lambda^0\bar{\Lambda}^0p)p$ by the R608 Collaboration at the ISR [50]. As seen in the proton-pomeron cms, there is in each case a forward Λ^0 in correlation with a backward K^+ or p, respectively, whereas the ϕ^0 and $\bar{\Lambda}^0$, which do not contain any proton valence quarks, show no such behaviour but are centrally produced. In particular the first reaction is a very suitable analyzer of the interaction mechanism since the fate of the proton valence quarks are well defined; a valence ud diquark goes forward and the remaining u valence quark is apparently back-scattered leading to a quark-diquark separation which hadronizes into the forward Λ^0, backward K^+ and central ϕ^0 by the creation of two $s\bar{s}$ pairs. This result is certainly in qualitative agreement with point-like pomeron-quark coupling used in the pomeron-photon analogy, but it may also be consistent with a pomeron-hadron picture having a $q\bar{q}$ component such that the $\bar{q}$ can annihilate a proton valence quark and the observed backward quark be viewed as a spectator from the pomeron. Independently of the details of these interpretations, however, the conclusion of an underlying partonic process in the pomeron-proton interaction seems unavoidable.

4.2 Hard diffractive scattering

If the pomeron has a parton substructure it may be possible to probe it in a hard scattering process [44] as, for example, between a gluon in the pomeron and a parton

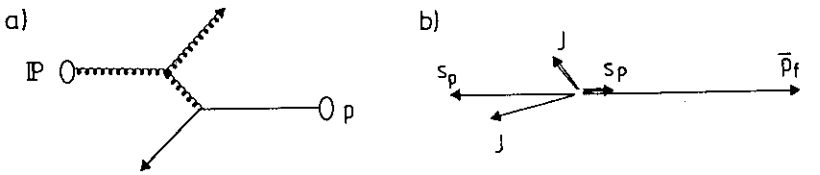

Figure 25: *(a) The hard parton-parton scattering subprocess in the pomeron-proton system, i.e. the lower vertex (or "blob") in Fig. 24a. (b) The topology of the scattering process as seen in the overall $p\bar{p}$ cms; $\bar{p}_f$ is the quasi-elastically scattered antiproton, J denotes the jets from the hard scattering and S denotes spectator jets. Double arrows are jets originating from the pomeron, while simple arrows are those from the proton.*

in the proton (Fig. 25a). This would give rise to a very characteristic event topology, as illustrated in Fig. 25b, with a quasi-elastically scattered particle and an opposite (in rapidity) system having two high-$p_\perp$ jets and two low-$p_\perp$ spectator jets from the non-interacting partons in the pomeron and proton respectively. Of course, for this jet-structure to be observable, the diffractive mass has to be large enough, i.e. colliders are needed (Table 2).

The process proceeds via the emission of a pomeron with a small momentum transfer (upper vertex in Fig. 24a), and one of its constituent partons then experience a hard scatter against a proton quark or gluon. Although the pomeron is often thought to interact coherently in the dominant low momentum transfer processes, one may assume an individual coupling of its constituents at the lower vertex because of the large momentum transfer at that vertex. Factorization allows the diffractive two-jet cross-section to be written [44]

$$\frac{d^2\sigma_{jj}}{dtdM_X^2} = \frac{d^2\sigma_{sd}}{dtdM_X^2} \cdot \frac{\sigma_{Pp\to jj}}{\sigma_{Pp\to X}} \tag{15}$$

The single diffractive cross-section, σ_{sd}, has been measured at the collider by UA4 [43] and can be parametrized as $\frac{d^2\sigma_{sd}}{dtdM_X^2} = \frac{6.8}{M_X^2}[e^{5.6t} + 0.04 \cdot e^{2t}]$. A 'pomeron-proton total cross-section' of $\sigma_{Pp\to X} \approx 1$ mb can be extracted from data using Regge analysis [51]. The pomeron-proton hard scattering into jets can be calculated in QCD

$$\sigma_{Pp\to jj}(M_X) = \int dx_1 dx_2 d\hat{t} \sum_{i,k} f_i(x_1, Q^2) G(x_2) \frac{d\hat{\sigma}_i^k}{d\hat{t}} \tag{16}$$

if a pomeron structure function, $G(x)$, is provided. This function is clearly unknown, but with the assumption of only gluons in the pomeron one may try different possibilities to investigate the sensitivity. A function like $xG(x) = 6x(1-x)$ would be expected if only two gluons share the pomeron momentum, or $xG(x) = 6(1-x)^5$ if the pomeron were a many-gluon system. The gluon distribution is in principle experimentally measurable because a change in its shape shifts the parton-parton cms with respect to the X cms, which in turn changes the distribution of the high-$p_\perp$ jets.

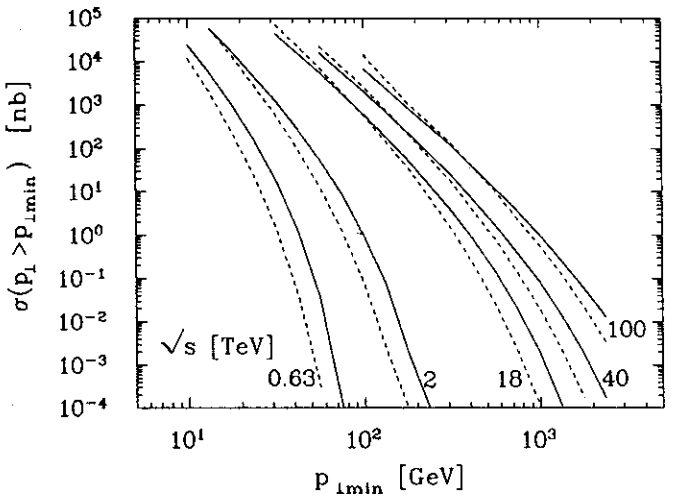

Figure 26: *Cross-section for diffractive events with jets having $p_\perp > p_{\perp min}$ in the region $|\eta| < 3$. The curves correspond to different $p\bar{p}$ collider energies and gluon structure functions of the pomeron given by $xG(x) = 6x(1-x)$ (full) and $6(1-x)^5$ (dashed).*

The resulting cross-sections for diffractive jet production are found to be quite large [44]. At the SPS collider the total cross-section for jets with $p_\perp \geq 8$ GeV is between 4 and 6×10^{-29} cm^2 depending on the pomeron structure function. Extrapolating to TeV energy colliders one obtains cross-sections as shown in Fig. 26. Since there are several uncertainties in this approach, see below, this naive extrapolation should not be taken too seriously, but rather as a first order of magnitude estimate. The expected major background process is given by normal QCD high-$p_\perp$ scattering where the spectator partons hadronize into a leading, diffractive-like proton with $x_F \geq 0.9$. At SPS energies, this process was estimated to have a cross-section two orders of magnitude below the diffractive jet signal [52]. This is, however, rather an upper limit since the uncertain elements of the beam jet fragmentation, as discussed above, tend to soften the beam jet.

These ideas are the starting point for 'hard diffraction' which has seen interesting developments since. First, heavy flavour production was considered [53] through gluon-gluon fusion into $Q\bar{Q}$ as the hard subprocess in the pomeron-proton interaction. The charm cross-section is, however, found to be far below the experimentally observed ones at the ISR. Due to the softness of the exchanged pomeron this is natural, since the available gluon-gluon cms energy is much lower than that for the same subprocess in non-diffractive proton-proton interactions, which is already below the data. The explanation for the large charm cross-sections at the ISR has to be sought elsewhere!

The theoretical basis for parton scatterings in the pomeron-proton interaction has furthermore been strengthened using Regge theory [54]. The important factorisation property is valid to the extent that Regge factorisation is valid in normal diffractive

scattering. Triple Regge theory and counting rules suggest a gluon structure function of the pomeron of the form $xg(x) = (0.18+5.46x)(1-x)$ which fulfills the momentum sum rule $\int_0^1 xg(x)\,dx = 1$. One should note that this is very close to the 'hard' structure function used as Ansatz and that the resulting phenomenology therefore will be the same. Based on the pomeron-photon analogy a different scheme has been proposed [55], in which the pomeron structure function is more similar to the photon structure function. Thus, a dominant $q\bar{q}$ structure is advocated with a structure function $xq(x) = 0.2x(1-x)$, which is normalised to $\int_0^1 xg(x)dx = 1/30$. Although the same shape as the simple 'hard' Ansatz is used, the hard diffractive cross-sections will be correspondingly reduced by this normalisation. The dominance of quarks rather than gluons would reduce the jet cross-sections further, due to the smaller colour charge, and exclude heavy flavour production in leading order, but would on the other hand give rise to other interesting processes like, e.g., Drell-Yan production of muon pairs and weak bosons at high enough diffractive masses. A quark substructure in the pomeron could also be directly measured in *ep* collisions at HERA, whereas a gluon structure would involve a more indirect, higher order process like photon-gluon fusion [44,56].

The idea of probing a possible pomeron parton structure by hard scattering processes has thus been well established. From a theoretical point of view it is hard to judge which of these scenarios is preferable and hence experimental information is needed to make progress. The UA8 collaboration has given preliminary results [57] which clearly hint at the existence of high-$p_\perp$ jets emerging from diffractively excited systems. The first indication of a smaller rate than expected should not be taken too literally since experimental jet finding problems were not included in the comparison with theoretical parton level calculations. A proper study is, however, in progress and the results will be most interesting, whichever way they will point!

5 Conclusions

Some important soft processes have been discussed in connection with the hard processes aiming at an understanding of the soft processes also in terms of a modern parton framework. This interplay between hard perturbative processes and soft hadronization is well developed for high-$p_\perp$ jets, which are well under control based on their production through leading order QCD Feyman diagram calculations, their perturbative evolution described by the parton cascade approach and finally their hadronization in terms of elaborate phenomenological models. The extrapolations to TeV colliders presented should therefore be taken seriously. Smaller discrepancies in comparison with future data may be cured by improving the models, but large ones would presumably indicate the occurrence of new physics phenomena!

Beam 'spectator' jets and minimum bias event structure cannot be considered understood, although models exist which are able to describe present energy data rather well. The increased activity, in terms of multiplicity and transverse momenta, with increasing energy seem to require some kind of multiple interactions, such as in the DTU approach or the new model based on perturbative QCD which can both be tuned to obtain good agreement with present data. The latter, although having some problems related to the cut-off against low-$p_\perp$ divergences, seems promising

since it provides a smooth transition to high-$p_\perp$ scattering. When extrapolating to future TeV collider energies a rather wide range of results are obtained due to the unknown energy dependence of some parameters in the models. Multiplicities are notoriously difficult to predict, whereas energy flows are more stable because of their smaller sensitivity to very soft particles.

Although the presently used fragmentation models work quite well in describing the experimental observations, the confinement problem is unsolved and therefore unconventional models are not excluded and some possibilities were mentioned. Therefore, this topic certainly leaves room for surprises!

In the field of diffractive scattering the discussion was concentrated on the new topic of 'hard diffraction' which was invented recently and had interesting developments. The notion of partons in the exchanged pomeron which can participate in hard scattering processes has become a theoretically realistic possibility and the first experimental indication for its occurence has been seen in terms of transverse energy clusters. This may lead to an exploration of the pomeron structure and its interactions in a parton level framework which provides an alternative, or perhaps complementary, treatment compared to the previous Regge analysis.

In conclusion, soft processes have for a long time been considered 'dirty' in the sense that a fundamental theory for proper calculations has been lacking. Nevertheless, they have many interesting aspects and are certainly very important for a general understanding of high energy interactions. New ideas and models are an important tool for improving our knowledge and crucial tests of their predictions will certainly involve, or even require, the higher energy interactions at future TeV colliders.

Acknowledgements. I am grateful to Dr. A. Ali for organizing an interesting workshop and a pleasant week in Erice.

References

[1] Z. Kunszt, E. Pietarinnen, Nucl. Phys. B164 (1980) 45, Phys. Lett. 132B (1983) 453
Z. Kunszt, W.J. Stirling, Phys. Lett. 171B (1986) 307 (and references therein).

[2] G. Ingelman, DESY 87–145, and in proc. XVth International Winter Meeting on Fundamental Physics, Sevilla, Spain, 1987.

[3] G.C. Fox, S. Wolfram, Nucl. Phys. B168 (1980) 285
R.D. Field, S. Wolfram, Nucl. Phys. B213 (1983) 65
T.D. Gottschalk, Nucl. Phys. B214 (1983) and CALT-68-1083
R. Odorico, Nucl. Phys. B228 (1983) 381

[4] G. Marchesini, B.R. Webber, Nucl. Phys. B238 (1984) 1
B.R. Webber, Nucl. Phys. B238 (1984) 492

[5] M. Bengtsson, T. Sjöstrand, Nucl. Phys. B289 (1987) 810

[6] G. Altarelli, G. Parisi, Nucl. Phys. B126 (1977)298
G. Altarelli, Phys. Rep. 81 (1982) 1

[7] A. Petersen et al., SLAC-PUB-4290
W. Hoffman, LBL 23922 and proc. Int. Symposium on Lepton and Photon Interactions at High Energies, Hamburg 1987.

[8] T. Sjöstrand, Phys. Lett. 157B (1985) 321

[9] R.D. Field, R.P. Feynman, Nucl. Phys. B136 (1978) 1

[10] G. Ingelman, Physica Scripta 33 (1986) 39

[11] D. Amati, G. Veneziano, Phys. Lett. 83B (1979) 87
A. Bassetto, M. Chiafoloni, G. Marchesini, Phys. Lett. 83B (1979) 207; Nucl. Phys. B163 (1980) 477

[12] C.-K. Ng, Phys. Rev. D31 (1985) 469

[13] B. Andersson, G. Gustafson, G. Ingelman, T. Sjöstrand, Phys. Rep. 97 (1983) 31

[14] T. Sjöstrand, Phys. Lett. 142B (1984) 420

[15] B. Andersson, G. Gustafson, B. Söderberg, Z. Phys. C20 (1983) 317

[16] I. Montvay, Phys. Lett. 84B (1979) 331

[17] C. Peterson, T.F. Walsh, Phys. Lett. 91B (1980) 455

[18] A. Drescher, Thesis, Inst. f. Physik der Universität Dortmund, January 1987
U. Matthiesen, Thesis, Inst. f. Physik der Universität Dortmund, January 1987

[19] W. Bartel et al., JADE collaboration, Z. Phys. C33 (1986) 23

[20] G. Kramer, B. Lampe, DESY 87-106

[21] N. Magnussen, private communication.

[22] G. Arnison et al., UA1 collaboration, Nucl. Phys. B276 (1986) 253

[23] P. Ghez, G. Ingelman, Z. Phys. C33 (1987) 465

[24] T. Åkesson et al., AFS collaboration, Z. Phys. C30 (1986) 27

[25] G. Ingelman, D.E. Soper, Phys. Lett. 148B (1984) 171

[26] P.N. Burrows, G. Ingelman, Z. Phys. C34 (1987) 91

[27] H.-U. Bengtsson, T. Sjöstrand, Comput. Phys. Commun. 46 (1987) 43

[28] T. Sjöstrand, Comput. Phys. Commun. 39 (1986) 347
T. Sjöstrand, M. Bengtsson, Comput. Phys. Commun. 43 (1987) 367

[29] B. Andersson, G. Gustafson, I. Holgersson, O. Månsson, Nucl. Phys. B178 (1981) 242

[30] E.A. De Wolf, in proc. XV International Symposium on Multiparticle Dynamics, Lund, June 1984. Eds. G. Gustafson, C. Peterson, World Scientific, p. 2

[31] P. Aurenche, F.W. Bopp, Phys. Lett. 114B (1982) 363
A. Capella, J. Tran Than Van, Phys. Lett. 114B (1982) 450; Z. Phys. C18 (1983) 85; ibid. C23 (1984) 165

[32] T. Sjöstrand, FNAL Pub-85/119-T

[33] T. Sjöstrand, M. van Zijl, Phys. Rev. D36 (1987) 2019.

[34] G.J. Alner et al., UA5 Collaboration, Phys. Lett. 138B (1984) 304

[35] C. Albajar et al., UA1 Collaboration, in proc. workshop on Physics Simulations at High Energies, Madison, Wisconsin 1986.

[36] B. Humpert, G. Ingelman, Int. conference 'Hadron Structure 83', Smolenice, Czechoslovakia 1983.

[37] H.U. Bengtsson, G. Ingelman, Comput. Phys. Commun. 34 (1985) 251

[38] G. Gustafson, Phys. Lett. 175B (1986) 453

[39] T.S. Biro, H.B. Nielsen, J. Knoll, Nucl. Phys. B245 (1984) 449

[40] L. van Hove, Z. Phys. C27 (1985) 135

[41] U. Amaldi, M. Jacob, G. Matthiae, Ann. Rev. Nucl. Sci. 26 (1976) 385
G. Alberi, G. Goggi, Phys. Rep. 74 (1981) 1
K. Goulianos, Phys. Rep. 101 (1983) 169

[42] F.E. Low, Phys. Rev. D12 (1975) 163
S. Nussinov, Phys. Rev. Lett. 34 (1975) 1286; Phys. Rev. D14 (1976) 246

[43] M. Bozzo et al., UA4 collaboration, Phys. Lett. 136B (1984) 217

[44] G. Ingelman, P.E. Schlein, Phys. Lett. 152B (1985) 256

[45] A. Donnachie, P. V. Landshoff, Nucl. Phys. B244 (1984) 322

[46] A.M. Smith et al., R608 Collaboration, Phys. Lett. 167B (1986) 248

[47] D.G. Richards, Nucl. Phys. B258 (1985) 267

[48] P.V. Landshoff, O. Nachtman, Z. Phys. C35 (1987) 405

[49] D. Bernard et al., Phys. Lett. 166B (1986) 459

[50] A.M. Smith et al., R608 Collaboration, Phys. Lett. 163B (1985) 267

[51] K.A. Ter-Martirosyan, Phys. Lett. 44B (1973) 179
A.B. Kaidalov, K.A. Ter-Martirosyan, Nucl. Phys. B75 (1974) 471
D.P. Roy, R.G. Roberts, Nucl. Phys. B77 (1974) 240

[52] G. Ingelman, proc. first Int. workshop on Elastic and Diffractive Scattering at the Collider and Beyond, Chateau Blois, France 1985, Eds. B. Nicolescu, J. Tran Than Van, Editions Frontières, p. 135

[53] H. Fritzsch, K.H. Streng, Phys. Lett. 164B (1985) 391

[54] E.L. Berger, J.C. Collins, D.E. Soper, G. Sterman, Nucl. Phys. B286 (1987) 704

[55] A. Donnachi, P.V. Landshoff, DAMTP 87/2, DAMTP 87/16

[56] N. Arteaga-Romero, P. Kessler, J. Silva, Mod. Phys. Lett. vol 1, No. 3 (1986) 211

[57] P.E. Schlein, in proc. XXIII International Conference on High Energy Physics, Berkeley 1986, Ed. S.C. Loken, World Scientific, vol II, p. 1331